Journal of Alloys and Compounds 509 (2011) 6609–6615

Contents lists available at ScienceDirect

Journal of Alloys and Compounds

journal homepage: www.elsevier.com/locate/jallcom

Electromagnetic properties of Ni and La doped strontium hexaferrites in the microwave region

C.A. Stergiou*, G. Litsardakis

Laboratory of Materials for Electrotechnics, Department of Electrical and Computer Engineering, Aristotle University, Thessaloniki, GR-54124, Greece

ARTICLE INFO

Article history:
Received 20 December 2010
Received in revised form 11 March 2011
Accepted 17 March 2011
Available online 29 March 2011

Keywords:
W-type hexaferrites
Complex permeability
Complex permittivity
Microwaves
Magnetocrystalline anisotropy

ABSTRACT

The complex permeability and permittivity spectra of novel Ni and La substituted $SrCo_2Fe_{16}O_{27}$ W-type hexaferrites are studied in the 2–18 GHz microwave band. While permittivity exhibits practically no dispersion in the specific testing frequency range, both doping elements yield an increase of dielectric polarization. The permeability of composite specimens is governed by the inherent tendency of Ni and La to induce the anisotropy transformation from planar to axial configuration. Actually, the decrease of the in-plane and out-of-plane anisotropy fields H_ϕ and H_θ, along with the high saturation magnetization M_s, for low substitution rates, result in the significant rising of μ''_{max} and its shift to substantially lower frequencies. Thus, the alteration of the Ni or La proportion enables the tuning of the magnetic loss peak over the range 5.8–16.7 GHz with maximum values as high as 0.85. Moreover, with the aim to investigate the impact of anisotropy on the dynamic magnetic properties, some essential formulations are reviewed. Through this analysis, the minimization of H_ϕ of the intermediate compounds in the vicinity of the anisotropy transition, which indicates the existence of an isotropic easy magnetization surface, is highlighted as a basic design requirement for the fabrication of soft hexagonal ferrites with increased μ' and μ'' values.

1. Introduction

Planar hexaferrites is a special group of hexagonal ferrites with a wide range of applications as its members possess interesting soft magnetic properties. Their valuable and useful quality stems from their strong magnetocrystalline anisotropy and the occurrence of the ferromagnetic resonance at higher frequencies, compared to those encountered in the spinel ferrites. Actually, the formulation of Snoek's limit for the case of planar hexaferrites allows them to retain high real permeability values in the microwave frequency range, until its degradation and the rise of magnetic losses in the vicinity of natural resonance [1]. Moreover, the composition-controlled variation of the permeability and permittivity spectra may be utilized for tuning the ferrites' properties through chemical manipulation. Therefore, apart from the advantageous coupling of the low-loss hexaferrites with strong uniaxial anisotropy to microwave signals [2], various compounds mainly based on planar Co–M, Co_2–Z, Co_2–W and Y-type hexaferrites are extensively employed for electromagnetic wave attenuation and interference suppression [3–6]. Among them, the $Ba(Sr)Co_2Fe_{16}O_{27}$ W-type hexaferrite, which displays the strongest in-plane anisotropy found for hexagonal ferrites [7], was used as the reference composition in several solid solution series. Specifically, $Ba(Sr)Co_xZn_{2-x}Fe_{16}O_{27}$ is undoubtedly the most widely studied W-type hexaferrite system, since numerous works report on the intermediate substances in an attempt to tailor their properties. Thus, it is inferred that the Zn substitution for Co, at a suitable proportion, may enhance saturation magnetization [7–10], and lead to the design of thinner and superior microwave absorbers in terms of bandwidth and reflection losses [11,12].

However, within the literature less attention was attracted to the Ni substitution for Co or La for Sr in the $SrCo_2$–W hexaferrite and particularly to the potential use of the resultant compounds as electromagnetic wave absorbers. In fact, the unique report on the electromagnetic characterization of hexaferrites $BaCo_xNi_{2-x}Fe_{16}O_{27}$ is confined to substitution rates $0 \le x \le 1.4$ in the Ka frequency band (26.5–40 GHz) [13]. Regarding the La containing Co_2–W hexaferrites, there are few published studies, which also solely refer to barium being substituted and either reject or ignore the dependence of the complex permeability on magnetocrystalline anisotropy [14,15]. The deficiencies of the relevant research necessitate further examination of the anisotropy transition from planar to uniaxial, which takes place at certain substitution proportion, and its impact on the electromagnetic behaviour. Hence, an attempt was initially made to fabricate pure samples of the Ni and La doped $SrCo_2$–W and deal with the insuffi-

* Corresponding author. Tel.: +30 2310 996384; fax: +30 2310 996302.
E-mail address: stergiou.babis@gmail.com (C.A. Stergiou).

0925-8388/$ – see front matter © 2011 Elsevier B.V. All rights reserved.
doi:10.1016/j.jallcom.2011.03.107

cient available data concerning the variation of the static magnetic properties (M_s, H_c) and anisotropy with the concentration of the substitution elements [16].

The scope of the present work is to complete the study of the new hexaferrite systems Sr(Co, Ni)$_2$–W and (Sr, La)Co$_2$–W, by investigating their electromagnetic properties in combination with the measured static properties and by probing into their relation to the magnetocrystalline anisotropy configuration. For this purpose a brief review on the essential theory-based formulations is also provided. The characterization of the dynamic properties of these novel materials renders more crucial since it enables the correlation of their macroscopic electromagnetic performance with their properties on the microscopic, crystal level and the evaluation of their efficiency in microwave absorbing applications.

2. Experimental

This study concerns the hexaferrite with the modified formula $Sr_{1.2}Co_{1.9}Fe_{15.8}O_{27+\delta}$ (SC), which is used as the reference compound, and two solid solution series of substituted ferrites, namely Ni doped compounds $Sr_{1.2}Co_{1.9-x}Ni_xFe_{15.8}O_{27+\delta}$ with $x = 0.5$, 0.95, 1.5, 1.9 (SN1, SN2, SN3, SN4) and La doped compounds $Sr_{1.2-y}La_yCo_{1.70}Fe_{16}O_{27+\delta}$ with $y = 0.05$, 0.10 (SL1, SL2). The hexaferrite samples were synthesized by the chemical coprecipitation method from nitrate salt precursors and are obtained as single phase with the exception of SN4 (Ni-spinel 2.8 wt%) after a composition optimization process [16].

For the microwave measurements composite samples containing 80 wt% (~43 vol%) of the sintered ferrite powders in polymer matrix were prepared. Actually, the ferrites were mechanically mixed with commercially available high density polyethylene micropowder and hot-pressed in an appropriate die to form toroidal specimens (outer diameter 7 mm, inner diameter 3.04 mm). The homogeneous dispersion of the ferrite particles with size range of 0.8–10 μm in the polymer matrix was verified by scanning electron microscopy observation. The composite rings were tightly fit in an N-type coaxial beadless airline and their S-parameters were measured over the frequency band of 2–18 GHz with the coaxial line technique, by using a full two-port calibrated HP8720C vector network analyzer. The desired thicknesses of the samples were set approximately to 2.5 mm to fulfill the conditions posed by the measurement method for the specific materials [17]. Eventually, the complex relative permittivity ($\varepsilon_r^* = \varepsilon_r' - j\varepsilon_r''$) and permeability ($\mu_r^* = \mu_r' - j\mu_r''$) of the composites were calculated from the S-parameters by implementing the Nicolson–Ross–Weir method [18,19], including the airgap and sample position corrections [17,20]. The relative uncertainties in the measurement of the electromagnetic properties were estimated as: $\Delta\mu'/\mu'' = 2\%$, $\Delta\mu''/\mu'' = 3\%$, $\Delta\varepsilon'/\varepsilon' = 3\%$ and $\Delta\varepsilon''/\varepsilon'' = 15\%$. This is further displayed by adding in brackets the respective absolute uncertainties of all the listed values.

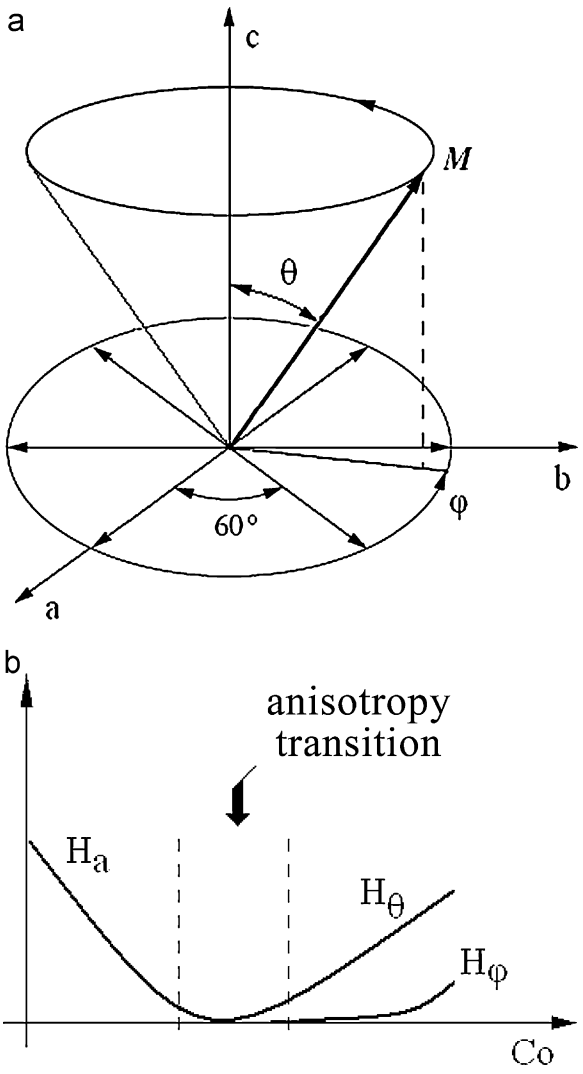

Fig. 1. (a) Potential anisotropy configurations (easy magnetization plane–cone-axis) and (b) estimated anisotropy fields variation with Co content.

3. Theoretical background

3.1. Magnetocrystalline anisotropy

Getting an insight into the electromagnetic properties of the produced compounds presupposes a review and clarification of the theoretical basis, regarding the magnetocrystalline anisotropy and ferromagnetic resonance in hexagonal ferrites. Specifically, the anisotropy originating from the hexagonal crystal structure is described by the anisotropy energy density (E_a), which is conventionally formulated as follows [21]:

$$E_a = k_1 \sin^2\theta + k_2 \sin^4\theta + k_3 \sin^6\theta + k_4 \sin^6\theta \cos(6\phi) \quad (1)$$

where θ, ϕ are the spherical coordinates of the magnetization vector M with respect to the z-axis lying parallel to the hexagonal c-axis (Fig. 1a) and k_i are the anisotropy constants. The changes in the magnitude and sign of k_i constants, which depend on the composition, temperature and the type of the crystal lattice, interconnect with the variation of magnetic ordering and anisotropy. By carrying out a mathematical analysis of the phenomenological definition of the energy E_a, in the common case where the sixth order constant k_4 is neglected, three possible types of anisotropy are discerned as corresponding to minimum energy directions, namely the uniaxial (easy magnetization c-axis), in-plane (easy a–b plane) and conical (easy conical surface) [22]. The anisotropy energy is usually quantified by the anisotropy field H_a, expressing the stiffness of magnetizing single crystals to saturation along the difficult magnetization directions, which for the case of uniaxial anisotropy is found:

$$H_a = \frac{2k_1}{\mu_0 M_s}, \quad k_1 > 0 \quad (2)$$

and for planar it becomes:

$$H_a = \frac{-2k_1 - 4k_2 - 6k_3}{\mu_0 M_s}, \quad -2k_1 - 4k_2 - 6k_3 > 0 \quad (3)$$

where M_s is the saturation magnetization.

Concerning the planar hexaferrites, while the compounds Zn$_2$–Y, Ni$_2$–Y or MnZn–Y display no pronounced anisotropy in the basal plane [23–25], the addition of Co^{2+} ions in other types of hexaferrites (W- and Z-type) has a marked influence on their in-plane anisotropic configuration [26]. Specifically, in ferrite compounds with even a relatively small Co content it is found that the constant k_4 should be taken into account as well. In this case, the term $k_4 \sin^6\theta \cos(6\phi)$, found in Eq. (1) of the anisotropy energy E_a, is responsible for the existence of a six-fold anisotropy on the a–b plane. Actually, since the anisotropy is additionally dependent on the angle ϕ on the basal plane, the energy $E_a(\theta, \phi)$ is interestingly minimized for $\phi = n\pi/3$ ($n = 0, 1, 2, \ldots$) and $\theta = \pi/2$ or $\theta = \theta_c$, where $\theta_c =$

$\sin^{-1}\left\{\left[\left(-k_2 \pm \left(\sqrt{k_2^2 - 3(k_3+k_4)k_1}\right)\right)/3(k_3+k_4)\right]^{1/2}\right\}$. Consequently, the preferred magnetization directions coincide with six equivalent axes separated by angles of 60°, which lie on the *a*–*b* plane or on the lateral surface of a cone with an angle $\theta = \theta_c$ to the *c*-axis (Fig. 1a).

Similarly to the anisotropy field H_a, the fields H_ϕ and H_θ are defined as measures of the stiffness of in-plane and out-of-plane magnetization rotation, respectively. When the easy magnetization directions are situated on the *a*–*b* plane ($\theta = \pi/2$) the anisotropy fields may be given as:

$$H_\phi = \frac{-36k_4}{\mu_0 M_s}, \quad k_4 < 0$$
$$H_\theta = \frac{-2k_1 - 4k_2 - 6k_3 - 6k_4}{\mu_0 M_s}, \quad 2k_1 + 4k_2 + 6k_3 + 6k_4 < 0 \tag{4}$$

While versions of Eqs. (2)–(4) appear in previous studies, it should be underlined that no respective equation has been formulated for any case of conical anisotropy ($\theta = \theta_c$). Besides, the possibility of the easy axes lying on a conical surface has not been raised elsewhere.

In general, the temperature and composition variation yield the spin reorientation transition between the aforementioned states of magnetic ordering. Thus, the W-type hexaferrites of the system Co_xZn_{2-x}–W exhibit the sequence of orientational phase transitions axis–cone-plane of easy magnetization with the increase of Co^{2+} concentration at room temperature, where the cobalt content *x* was found to promote the conical anisotropy when it varies in the range 0.7–0.9 [27] or 0.5–0.7 [10]. However, the existence of the intermediate preferred cone of easy magnetization is ignored in other studies of the systems Co_xZn_{2-x}–W [7,9] and Co_xNi_{2-x}–W [28]. From the general calculated magnetic phase diagrams [27] it is inferred that the axial anisotropy practically changes when the first order constant k_1 gets negative, since k_2 and k_3 are small compared to k_1 at room temperature. The minimization of $|k_1|$ in the vicinity of the phase transition results in the minimization of the anisotropy fields H_a and H_θ according to the Eqs. (2)–(4). Specially for the hexaferrite systems containing Co a qualitative diagram of anisotropy fields variation with Cobalt concentration is suggested in Fig. 1b, based on anisotropy measurements [10,29]. The observed trend of H_ϕ is attributed to the decrease of the negative constant k_4 with Co [7].

Regarding the particular hexaferrite systems under study, past anisotropy measurements and calculations were only performed on the end member hexaferrites. Hence, polycrystalline samples of $SrCo_2$–W and Ba(Sr)Ni_2–W were separately investigated and the anisotropy fields H_θ and H_a were measured to be 2.8 kOe [30] and 11.8–14.9 kOe [30–33], respectively. Nevertheless, there are no directly comparable values of the in-plane anisotropy field H_ϕ for Ba(Sr)Co_2–W ferrite or any information at all about the anisotropy field values of the La doped Ba(Sr)Co_2–W ferrite reported in the literature. Still, individual studies showed that H_ϕ is 2 to 10 times smaller than H_θ [7,10] and clear evidence are given of the decrease of H_θ with the addition of La in Ba(Sr)Co_2–W [16]. This qualitative and quantitative assessment of the magnetocrystalline anisotropy and spin orientation transition is rather crucial for the study of ferrites' electromagnetic behaviour since the ferromagnetic resonance and permeability spectra are decisively conditioned by the anisotropy configuration.

3.2. Dynamic magnetic properties

The ferromagnetic resonance, as a response of ferromagnetic materials to ac excitation, is the most important loss mechanism at microwave frequencies. This macroscopic phenomenon occurs at the characteristic frequency f_R which is mainly determined by the magnetocrystalline anisotropy of the samples. Assuming a six-fold in-plane anisotropy arrangement (*x*–*y* plane) and the *x*-axis being the reference easy magnetization direction of the material, the resonance frequency is derived from the equation:

$$f_R = \frac{\gamma}{2\pi}\sqrt{[H_\theta + (N_z - N_x)M_s][H_\varphi + (N_y - N_x)M_s]} \tag{5}$$

where H_θ and H_ϕ are the anisotropy fields defined in Eq. (4), γ is the gyromagnetic constant and $N_{x,y,z}$ are the demagnetizing factors. The definition of Eq. (5) stems from two seemingly different formulations [24,25], which coincide if we equate the orthogonal (*x*, *y*, *z*) coordinate system to the (*a*, *b*, *c*) crystallographic system and consider the proper signs of the anisotropy constants k_i. Similarly, for a material with axial anisotropy where *z*-axis is the preferred magnetization direction and by applying the appropriate axes transformation, the resonance frequency is given by:

$$f_R = \frac{\gamma}{2\pi}\sqrt{[H_a + (N_y - N_z)M_s][H_a + (N_x - N_z)M_s]} \tag{6}$$

As concerns the complex permeability μ^*, which originates from the precession of magnetic moment under an ac magnetic field, it also exhibits strong dependence on the anisotropy. In fact, for the static permeability μ_s' of isotropic polycrystalline samples the following expressions were obtained [1]: $\mu_s' - 1 \propto M_s^2/k_1$ for uniaxial anisotropy and $\mu_s' - 1 \propto M_s/H_\varphi$, for planar anisotropy. Since the imaginary part of permeability μ'' is proportional to the static magnetic susceptibility $\chi_s' = \mu_s' - 1$ [4] a similar relation to anisotropy is expected. That was expressed in previous studies of hexaferrites with axial [34] and planar anisotropy, where additionally the complex permeability spectrum was found to be dominated by its component on the basal plane [35,36].

4. Electromagnetic properties

The electromagnetic properties of the composite samples filled with the Ni and La substituted $SrCo_2$–W ferrite powders were measured in the frequency range 2–18 GHz. Since the macroscopic constitutive properties of the composites are dominated by the respective intrinsic properties of the ferrite filler, this investigation elucidates the relative trends in properties of the powders in connection with their chemical composition. Moreover, the knowledge of the complex permittivity and permeability further facilitates the direct assessment of the performance of practical planar devices employing the specific composite materials.

4.1. Complex permittivity

Initially, the complex permittivity $\varepsilon^*(f)$ spectra of the composites show practically no frequency dispersion effects. The lossy part of permittivity ε'', especially of the Ni doped samples, is not appropriate for extracting reliable conclusions due to the high fluctuation compared to the low level of the recorded values (from 0 to 0.16). On the other hand, the real part of permittivity ε' for the two series of substitutions appears to increase with the Ni and La content, as it is displayed in Fig. 2 a and b. The absolute uncertainty of this measurement is approximately 0.2, while the observed distances between the upper and the lower curves are further apart. Therefore, the specific sorting order of the ε' data series, which is retained throughout the monitored frequency band, cannot be ignored. Actually, this trend is justifiable, as in the Ni containing ferrites the oxidation mechanism $Ni^{2+} \leftrightarrow Ni^{3+}$ occurs in addition to the common reduction mechanism $Fe^{3+} \leftrightarrow Fe^{2+}$ [37]. Likewise, the La^{3+} substitution for Sr^{2+} in hexaferrites is associated with a valence change of Fe^{3+} ions through the indicative reaction $Sr^{2+} + Fe^{3+} \rightarrow La^{3+} + Fe^{2+}$ [15,38,39]. Thus, both substitution elements are expected to induce an increase of the electric

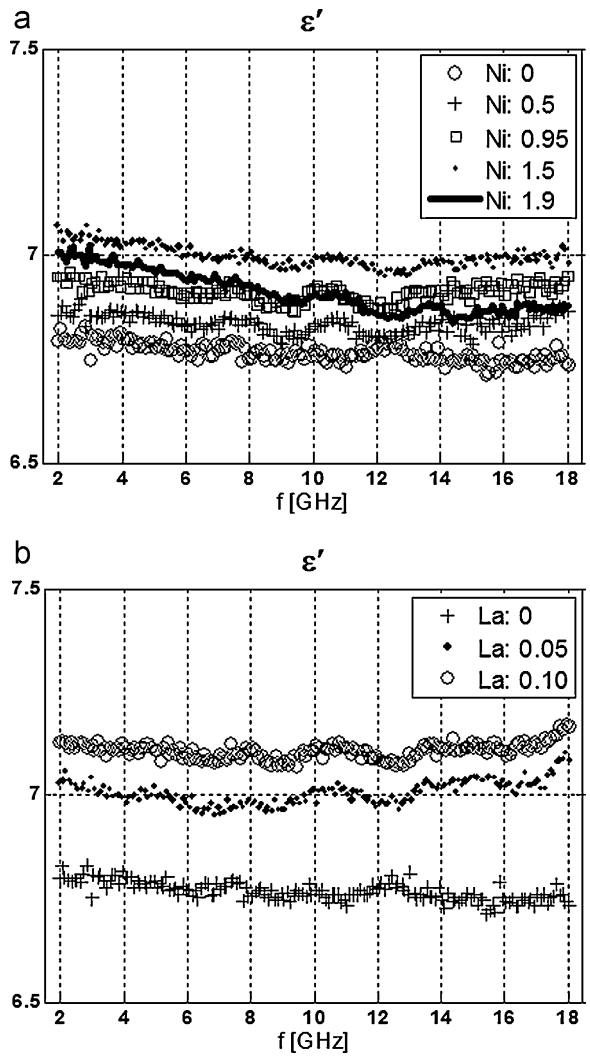

Fig. 2. Real part of permittivity ε' spectra for the composites of the hexaferrite system: (a) Sr(Co, Ni)–W and (b) (Sr, La)Co_2–W.

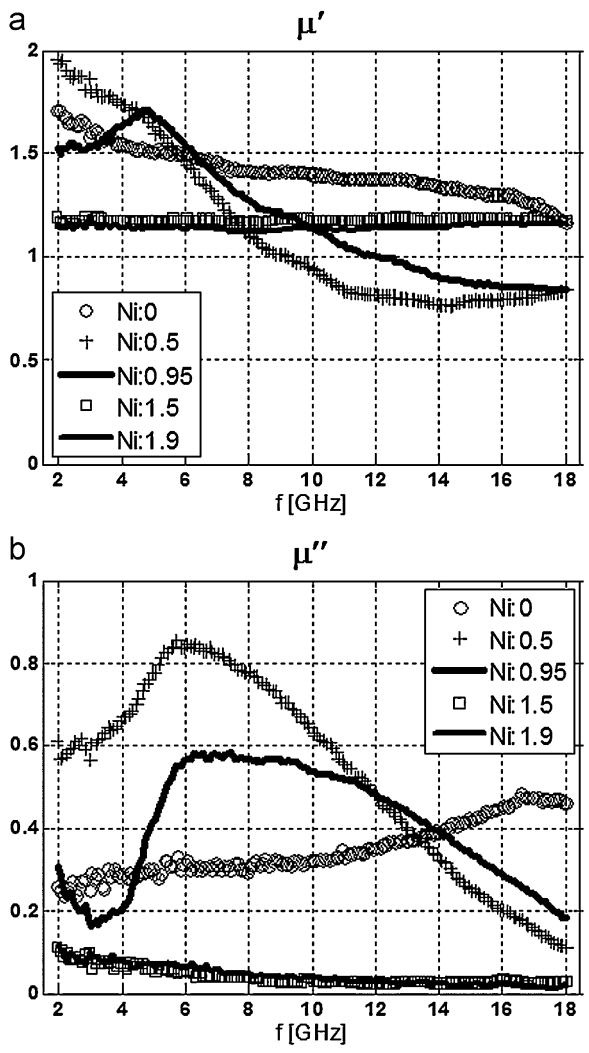

Fig. 3. Complex permeability spectra ($\mu^* = \mu' - j\mu''$) for the composites of the hexaferrite system Sr(Co, Ni)–W.

dipoles concentration due to the local charge imbalance, which enhances the dielectric polarization through the dipolar-rotational mechanism. This finally yields higher dielectric constant for the substituted compounds, compared to the undoped sample SC. As an exception, the dielectric properties of the fully substituted ferrite SN4 seem to be inferior to sample SN3, possibly because of the traced spinel $NiFe_2O_4$ impurity (~2.8 wt%). Moreover, it is suggested that even a small La proportion suffices to exceed the maximum permittivity achieved with Ni doping, which probably arises from the additional dipoles due to the physical dissimilarities between Sr and La, in terms of their valence, atomic weight and ionic radius.

4.2. Complex permeability

Figs. 3 and 4 depict the measured complex relative permeability spectra ((a) real part μ' and (b) imaginary part μ'') of the samples, which are determined by the intrinsic properties of the magnetic filler and most of which present the typical damped ferromagnetic resonance dispersion of composite ferrites. Since the ferrite powders employed comprise mainly multiple magnetic domain particles [16], a significant additional contribution of the domain wall resonance to the permeability is also anticipated. However, this phenomenon is located at frequencies lower than the specific testing frequency band (2–18 GHz).

With regard to the system of Ni doped hexaferrites $Sr_{1.2}Co_{1.9-x}Ni_xFe_{15.8}O_{27+\delta}$, the addition of Ni induced an initial decrease of the frequency of maximum losses $f\{\mu''_{max}\}$, originating from the ferromagnetic resonance, down to 5.8 GHz followed by an increase to 7.5 GHz, as it is shown in Table 1. For higher Ni content ($x \geq 1.5$) the materials exhibit harder magnetic characteristics and the μ'' peak is believed to appear at frequencies above 18 GHz. This observation is in accordance with the measured coercivity H_c [16], both indicating the occurrence of anisotropy transition for Ni content between 0.5 and 0.95, as it is described in Fig. 1b. Thus, the frequency $f\{\mu''_{max}\}$ of the planar hexaferrite sample SC decreases with the Ni substitution for Co as both in-plane and out-of-plane anisotropy fields diminish (H_θ and H_ϕ in Eq. (5)), reaches a minimum when the anisotropy fields are minimized and then increases again as the axial anisotropy develops and keeps

Table 1
Magnetic loss peaks of the hexaferrite system Sr(Co, Ni)–W.

Sample	Ni	$f\{\mu''_{max}\}$ [GHz]	μ'' (f)
SC	0	16.7	0.48 (3)
SN1	0.50	5.8	0.85 (2)
SN2	0.95	7.5	0.58 (2)
SN3	1.50	>18	–
SN4	1.90	>18	–

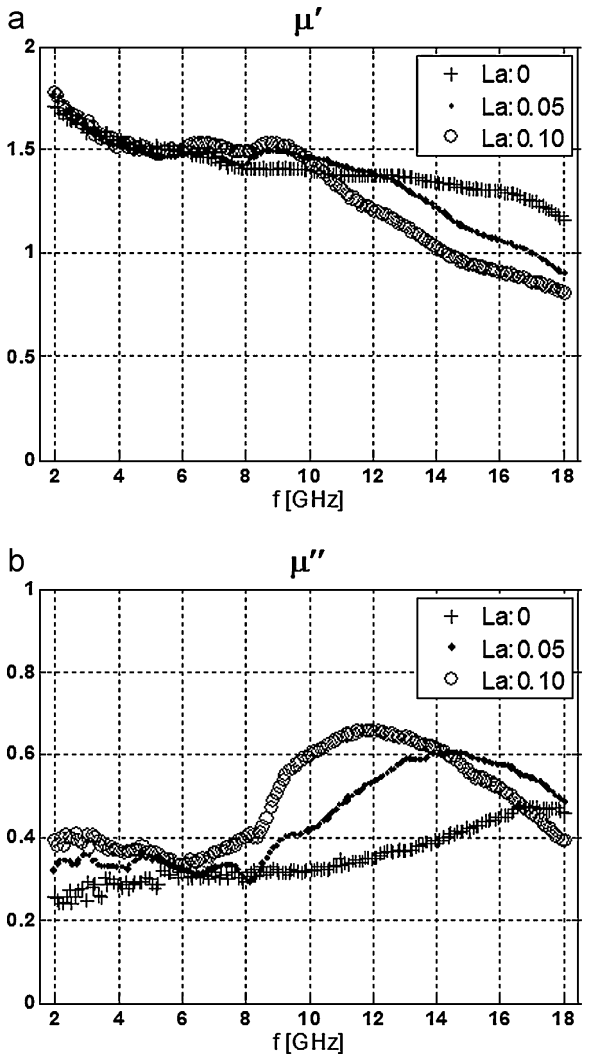

Fig. 4. Complex permeability spectra ($\mu^* = \mu' - j\mu''$) for the composites of the hexaferrite system (Sr, La)Co_2–W.

strengthening (H_a in Eq. (6)). The absence of any resonance-related peak in the 2–18 GHz band for the highly Ni doped W hexaferrites with $x = 1.5$ and 1.9 agrees with its location at the frequencies 32–37 GHz for $BaNi_2$–W [13,33].

By comparing the complex permeability values at $f\{\mu''_{max}\}$, an increase is noticed from $x = 0$ to 0.5 and thereafter μ' and μ'' are degrading. Taking into account the measured M_s of the respective powders [16] and the dependence of the permeability on the saturation magnetization and anisotropy fields, it is inferred that the composites with $x = 0.5$ and 0.95 exhibit correspondingly in-plane and axial anisotropy weaker than that of the planar undoped sample SC. Besides, $SrCo_2$–W compound was found to have the highest planar anisotropy among hexaferrites [7]. Hence, the maximum losses among the system Sr (Co, Ni)–W, which are recorded for the composite SN1 with $x = 0.5$, are attributed to the simultaneous minimization of the anisotropy on the easy magnetization surface along with the retention of strong saturation magnetization.

The complex permeability $\mu^*(f)$ measurements of the hexaferrite system (Sr, La)Co_2–W (Fig. 4) reveal the decrease of the frequency $f\{\mu''_{max}\}$ of the composite materials with La gradually from 16.7 to 11.8 GHz (Table 2). The addition of La in hexaferrites is known to correlate with the enhancement of the first order anisotropy constant k_1 through the formation of Fe^{2+} cations [40–42]. For low La doping in the planar hexaferrite SC the constant

Table 2
Magnetic loss peaks of the hexaferrite system (Sr, La)Co_2–W.

Sample	La	$f\{\mu''_{max}\}$ [GHz]	$\mu''(f)$
SC	0	16.7	0.48 (3)
SL1	0.05	14.6	0.61 (2)
SL2	0.10	11.8	0.66 (2)

k_1 is expected to increase yet remaining negative, thus diminishing the magnitude of the out-of-plane anisotropy H_θ (Eq. (4)) and possibly of the in-plane anisotropy H_ϕ too. Consequently, lowering of the frequency of the maximum losses occurs according to the Eq. (5). The initial weakening of the anisotropy with the La content is consistent with the reduction of the measured coercivity [16], and apparently accounts for the observed decrease of $f\{\mu''_{max}\}$ in La doped $BaCo_2$–W hexaferrites as well [15]. The recorded shift of the μ'' peak with the addition of La in the samples under study is in direct contradiction to what is reported in [14], where the specific high La doping is declared not to have any impact on the magnetocrystalline anisotropy of $BaCo_2$–W ferrite.

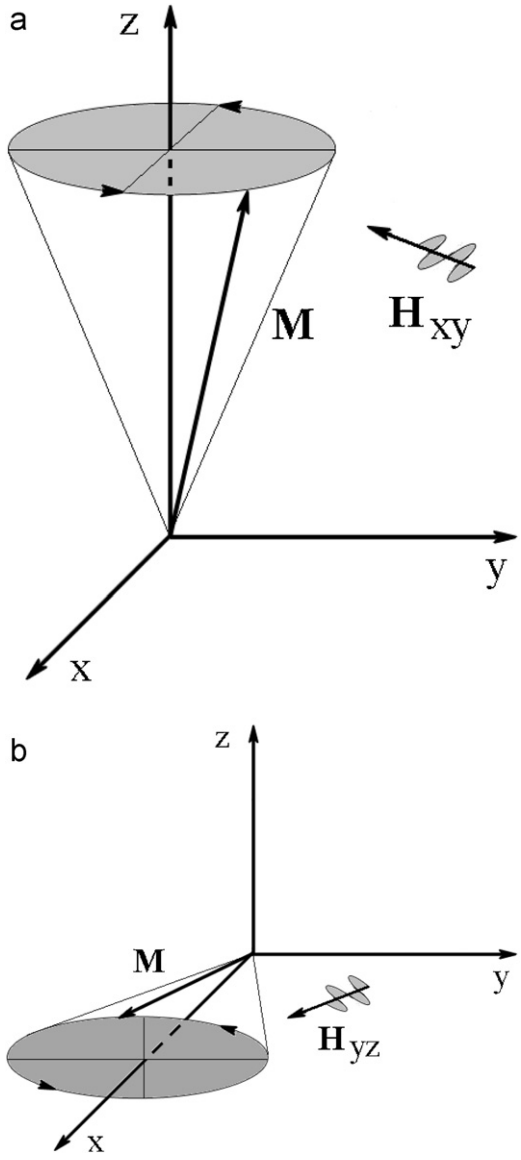

Fig. 5. Precession of magnetic moment M assuming (a) uniaxial anisotropy (easy z-axis) and (b) planar anisotropy (easy x-axis).

The La substitution for Sr in $SrCo_2$–W hexaferrites also effects an increase of maximum losses, as it is noticed in Fig. 4 and Table 2. This discernible rising of μ''_{max} cannot be fully ascribed to the measured magnetization variation, therefore gives additional clear evidence of the decrease of the in-plane anisotropy H_ϕ. Finally, in both substitution series Sr(Co, Ni)–W and (Sr, La)Co_2–W the competitive behaviour between the permeability and the resonance frequency is displayed, in accord with the well known Snoek's law and the recently stated constraints for the dynamic properties of composites containing planar hexaferrites [43,44].

5. Discussion

The investigation of the complex permeability spectra puts in evidence that, contrary to the widely held view, the demand for strong magnetic polarization and losses is satisfied to a higher extent away from the typical planar anisotropy arrangement. Specifically the existence of the six equivalent easy magnetization axes on the basal plane and the nontrivial anisotropy field H_ϕ hinder the motion of the magnetic moment and induce an elliptical precession, as it is depicted in Fig. 5 and has also been suggested in [45]. Hence, in pursuit of better soft magnetic materials the objective should rather be an isotropic easy magnetization surface than attaining the specific planar geometry. Although the actual angle between the *c*-axis and magnetic moment is a matter of dispute in the literature for the Ba(Sr)Co_2–W hexaferrites, the unimpeded motion of the magnetic moment even on a conical-shaped surface theoretically enhances the response of the material to ac excitation, therefore increases the real and imaginary part of permeability μ' and μ'' which originate from this magnetization mechanism.

This is the issue with the samples SN1 (Ni: 0.50) and SL2 (La: 0.10), where H_ϕ is believed to be minimized just before the transition from planar to uniaxial anisotropy occurs. Thus, μ' values as high as 1.51(3) and 1.24(3) and μ'' up to 0.85(2) and 0.66(2) were measured for SN1 and SL2, respectively. While there is no measure available to assess the dynamic magnetic properties of the system Sr(Co, Ni)–W, the (Sr, La)Co_2–W system possesses comparable μ' values and superior losses to the corresponding quantities of the (Ba, La)Co_2–W system [15], despite the considerably lower filling factor of the composites fabricated in the present study.

6. Conclusion

New Ni and La doped $SrCo_2$–W hexaferrites were investigated in terms of their electromagnetic properties in the microwave frequency range from 2 to 18 GHz. The complex permittivity spectra demonstrate practically no variation in the specific testing frequency band, while dielectric polarization appears to increase with the Ni and La content, as a result of the enhanced dielectric dipoles concentration. Concerning the dynamic magnetic properties, the observed increase of μ''_{max} and its shift to lower frequencies for small substitution rates consort with the inherent tendency of both substituting elements towards the transition from planar to uniaxial anisotropy. Actually, the main features spotted were the decrease of the characteristic frequency $f\{\mu''_{max}\}$ from 16.7 GHz (undoped $SrCo_2$–W) to 5.8 GHz (Ni: 0.50) and 11.8 GHz (La: 0.10) and the increase of the magnetic losses μ'' from 0.48(3) (undoped $SrCo_2$–W) to 0.85(2) (Ni: 0.50) and 0.66(2) (La: 0.10). Thus, both ferrite systems enable the composition-controlled tuning of their relatively strong loss peaks over a notably wide frequency range.

In addition to the characterization of the new materials itself, this investigation summarizes and clarifies, where needed, the explicit dependence of the complex permeability features on the static magnetic properties and magnetocrystalline anisotropy of ferrites. Based on these formulations, it highlights the significance of the reduced in-plane anisotropy H_ϕ displayed by the compositions in the vicinity of the anisotropy transition, before the appearance of uniaxial arrangement. In these compounds the minimized H_ϕ favours the unhindered motion of the magnetic moment on a surface and causes μ' and μ'' to increase. Therefore, the basic requirement for efficient soft ferrites is rephrased to exclude strictly geometrical aspects and to focus on the existence of an isotropic easy magnetization surface, possibly of conical shape.

In conclusion, an insight into the dynamic magnetic properties of planar hexaferrites is provided and the design guidelines are set in order to develop, not only efficient microwave absorbers, but high permeability materials in microwaves as well. The present research further indicates that the fabricated group of Ni and La doped W-hexaferrite composites comprises lossy materials which could be interestingly employed in the design of new microwave absorbing structures particularly in the 6–14 GHz range.

Acknowledgements

This paper is a part of the 03ED742 research project, implemented within the framework of the "Reinforcement Programme of Human Research Manpower" (PENED) and co-financed by National and Community Funds (25% from the Greek Ministry of Development-General Secretariat of Research and Technology and 75% from E.U.-European Social Fund). The authors wish to thank Assistant Professor T. Yioultsis for substantial help with electromagnetic measurements.

Appendix A. Supplementary data

Supplementary data associated with this article can be found, in the online version, at doi:10.1016/j.jallcom.2011.03.107.

References

[1] S. Chikazumi, Physics of Magnetism, Wiley, 1964.
[2] V.G. Harris, A. Geiler, Y. Chen, S. Yoon, M. Wu, A. Yang, Z. Chen, P. He, P. Parimi, X. Zuo, C. Patton, M. Abe, O. Acher, C. Vittoria, J. Magn. Magn. Mater. 321 (2009) 2035–2047.
[3] P. Singh, V.K. Babbar, A. Razdan, S.L. Srivastava, V.K. Agrawal, T.C. Goel, J. Mater. Sci. 41 (2006) 7190–7196.
[4] Z.W. Li, L. Guoqing, L. Chen, W. Yuping, C.K. Ong, J. Appl. Phys. 99 (2006) 063905.
[5] A. Oikonomou, T. Giannakopoulou, G. Litsardakis, J. Magn. Magn. Mater. 316 (2007) e827–e830.
[6] H.J. Kwon, J.Y. Shin, J.H. Oh, J. Appl. Phys. 75 (10) (1994) 6109–6111.
[7] H. Graetsch, F. Haberey, R. Leckebusch, M.S. Rosenberg, K. Sahl, IEEE Trans. Magn. 20 (3) (1984) 495–500.
[8] V.D. Reddy, P.V. Reddy, Phys. Status Solidi A 142 (1994) 451–458.
[9] X. Wang, T. Ren, L. Li, L. Zhang, J. Magn. Magn. Mater. 184 (1) (1998) 95–100.
[10] Z.W. Li, L. Chen, C.H. Ong, J. Appl. Phys. 94 (9) (2003) 5918–5924.
[11] Z. Haijun, Y. Xi, Z. Liangying, Ceram. Int. 28 (2002) 171–175.
[12] Z.W. Li, L. Chen, Y. Wu, C.K. Ong, J. Appl. Phys. 96 (1) (2004) 534–539.
[13] Y.J. Kim, S.S. Kim, IEEE Trans. Magn. 38 (5) (2002) 3108–3110.
[14] G. Shen, Z. Xu, Y. Li, J. Magn. Magn. Mater. 301 (2) (2006) 325–330.
[15] L. Hongying, Z. Haifeng, Y. Lanying, X. Jijing, G. Shucai, M. Jian, H. Guangyan, J. Rare Earth 25 (2007) 590–595.
[16] C.A. Stergiou, G. Litsardakis, Preparation and magnetic characterization of strontium hexaferrites doped with Ni and La, unpublished results.
[17] A Guide to Characterisation of Dielectric Materials at RF and Microwave Frequencies, Institute of Measurement and Control – National Physical Laboratory, London, 2003.
[18] A.M. Nicolson, G.F. Ross, IEEE Trans. Instrum. Meas. 19 (4) (1970) 377–382.
[19] W.B. Weir, IEEE Proc. 62 (1) (1974) 33–36.
[20] J. Baker-Jarvis, M.D. Janezic, B.F. Riddle, R.T. Johnk, P. Kabos, C.L Holloway, R.G. Geyer, C.A. Grosvenor, Measuring the permittivity and permeability of lossy materials: Solids, Liquids, Metals, Building Materials and Negative-Index Materials, Natl. Inst. Stand. Technol., Tech. Note 1536, February 2005.
[21] J. Smit, H.P.J. Wijn, Ferrites, Wiley, New York, 1959.
[22] G. Asti, F. Bolzoni, J. Magn. Magn. Mater. 20 (1980) 29–43.
[23] A.A. Oshlakov, V.A. Zhuravlev, Russ. Phys. J. 43 (9) (2000) 804–807.
[24] O. Kohmoto, J. Magn. Magn. Mater. 310 (2007) 2561–2562.
[25] M. Obol, C. Vittoria, J. Magn. Magn. Mater. 272–276 (2004) e1799–e1800.
[26] R.A. Braden, I. Gordon, R.L. Harvey, IEEE Trans. Magn. MAG-2 (1) (1966) 43–47.
[27] S.M. Zhiyakov, E.P. Naiden, G.I. Ryabtsev, Russ. Phys. J. 35 (9) (1993) 800–805.

[28] A.M. Abo El Ata, M.K. El Nimr, D. El Kony, A.H. Al-Hammadi, J. Magn. Magn. Mater. 204 (1–2) (1999) 36–44.
[29] E.P. Naiden, V.I. Maltsev, G. Ryabtsev, Phys. Status Solidi A 120 (1990) 209–220.
[30] F. Leccabue, R. Panizzieri, G. Albanese, G. Leo, N. Suarez Almodovar, Mater. Res. Bull. 23 (2) (1988) 263–275.
[31] T. Besagni, A. Deriu, F. Licci, L. Pareti, S. Rinaldi, IEEE Trans. Magn. 17 (6) (1981) 2636–2638.
[32] F. Licci, L. Pareti, S. Rinaldi, J. Appl. Phys. 52 (3) (1981) 2526–2528.
[33] N.E. Kazantseva, A.T. Ponomarenko, V.G. Shevchenko, C. Klason, Electromagnetics 20 (2000) 453–466.
[34] T. Kagotani, D. Fujiwara, S. Sugimoto, K. Inomata, M. Homma, J. Magn. Magn. Mater. 272–276 (1) (2004) e1813–e1815.
[35] V.A. Zhuravlev, Russ. Phys. J. 32 (1) (1989) 33–36.
[36] V.A. Zhuravlev, Russ. Phys. J. 40 (2) (1997) 167–171.
[37] A.M. Abo El Ata, M.K. El Nimr, D. El Kony, A.H. Al-Hammadi, J. Magn. Magn. Mater. 202 (1999) 397–404.
[38] X. Liu, W. Zhong, S. Yang, Z. Yu, B. Gu, Y. Du, Phys. Status Solidi A 193 (2) (2002) 314–319.
[39] S. Ounnunkad, Solid State Commun. 138 (2006) 472–475.
[40] J. Kui, H. Lu, Y. Du, J. Magn. Magn. Mater. 31–34 (1983) 801–802.
[41] F.K. Lotgering, P.R. Locher, R.P. Van Stapele, J. Phys. Chem. Solids 41 (1980) 481–487.
[42] M. Küpferling, R. Grössinger, M.W. Pieper, G. Wiesinger, H. Michor, C. Ritter, F. Kubel, Phys. Rev. B 73 (2006) 144408.
[43] A.L. Adenot, O. Acher, T. Taffary, L. Longuet, J. Appl. Phys. 91 (10) (2002) 7601–7603.
[44] A.N. Lagarkov, N. Rozanov, J. Magn. Magn. Mater. 321 (14) (2009) 2082–2092.
[45] H. How, X. Zuo, C. Vittoria, IEEE Trans. Magn. 41 (8) (2005) 2349–2354.